Tumor uptake of radiolabeled acetate reflects the expression of cytosolic acetyl-CoA synthetase: implications for the mechanism of acetate PET

Tumor uptake of radiolabeled acetate reflects the expression of cytosolic acetyl-CoA synthetase: implications for the mechanism of acetate PET

Yukie Yoshii[a], Atsuo Waki[a], Takako Furukawa[b], Yasushi Kiyono[a], Tetsuya Mori[a,c], Hiroshi Yoshii[d], Takashi Kudo[a], Hidehiko Okazawa[a], Michael J. Welch[c], Yasuhisa Fujibayashi[a,b,*]

[a]*Biomedical Imaging Research Center, University of Fukui, Eiheiji, Fukui 910-1193, Japan*

[b]*Molecular Imaging Center, National Institute of Radiological Sciences, Anagawa, Chiba 263-8555, Japan*

[c]*Mallinckrodt Institute of Radiology, Washington University School of Medicine, St. Louis, Missouri 63110, USA*

[d]*Department of Biochemistry and Bioinformative Science, Faculty of Medical Sciences, University of Fukui, Eiheiji, Fukui 910-1193, Japan*

*Corresponding author: Yasuhisa Fujibayashi, Biomedical Imaging Research Center, University of Fukui, 23-3, Shimoaizuki, Eiheiji, Fukui 910-1193, Japan. Tel.: +81-776-61-8491; fax: +81-776-61-8170. *E-mail address*: yfuji@u-fukui.ac.jp (Y. Fujibayashi).

Abbreviated title: Mechanism of tumor acetate uptake

Key words: Acetate; Acetyl-CoA synthetase; PET; Hypoxia; Tumor

Abstract

Introduction: [1-^{11}C]acetate positron emission tomography (PET) is used for myocardial studies. In the myocardium, mitochondrial acetyl-CoA synthetase (ACSS1) mainly contributes to the radiopharmaceutical uptake. [1-^{11}C]acetate PET is also used for tumor diagnosis; however, the uptake mechanism of radiolabeled acetate in tumors remains unclear. Our previous study reported that cytosolic acetyl-CoA synthetase (ACSS2) was expressed in tumor cells and up-regulated under hypoxia; whereas, expression of ACSS1 was negligible regardless of the oxygen conditions. We also indicated that ACSS2 is a bi-directional enzyme that controls acetyl-CoA / acetate metabolism in tumor cells. In this study, to elucidate the basic mechanism of tumor acetate uptake, we focused on ACSS2 and investigated the role of ACSS2 in the uptake of radiolabeled acetate in tumor cells.

Methods: [1-^{14}C]acetate uptake and ACSS2 expression were examined in four tumor cell lines under normoxia or hypoxia. An ACSS2 knockdown study was also performed.

Results: [1-^{14}C]acetate uptake was increased in the tumor cells under hypoxia. This pattern followed that of ACSS2 expression. The incorporated ^{14}C was mostly distributed in the lipid-soluble fractions, and this tendency increased under hypoxia. ACSS2 knock down led to a corresponding reduction in [1-^{14}C]acetate uptake in all tumor cell lines examined under normoxia and hypoxia.

Conclusions: ACSS2 plays an important role in the uptake of radiolabeled acetate in tumor cells, which is different from that in the myocardium, which mainly involves ACSS1. The uptake of radiolabeled acetate in tumors increased under hypoxia along with up-regulation of ACSS2 expression. This suggests a possible mechanism for acetate PET for tumors.

1. Introduction

[1-^{11}C]acetate positron emission tomography (PET) is used for the evaluation of myocardial blood flow and oxidative metabolism [1-4]. In the myocardium, the uptake mechanism of radiolabeled acetate is well-understood, i.e., the acetyl-CoA synthetase (ACSS, EC 6.2.1.1; ATP + acetate + CoA ↔ AMP + diphosphate + acetyl-CoA) distributed in mitochondria (termed ACSS1 in this study) is highly expressed compared with that distributed in the cytosol (termed ACSS2) and contributes to uptake of radiolabeled acetate [5-7]. It was also demonstrated that the radiolabeled acetate incorporated by the heart is mainly used for oxidation and metabolized into CO_2 via the TCA cycle, but is also partly used for lipid synthesis [5, 8-11].

[1-^{11}C]acetate PET has also become a useful tool for detecting various kinds of malignant tumors, e.g., prostate cancer [12, 13], renal carcinoma [14], hepatocellular carcinoma [15], brain astrocytoma [16], and glioma [17]. Alternatively, [^{18}F]fluoroacetate is being developed as an analog of [1-^{11}C]acetate [18, 19] and has been shown to be useful for detecting prostate cancer by PET studies [20, 21]. However, information on the exact uptake mechanism of radiolabeled acetate in tumor cells is limited.

So far, several studies on the uptake of radiolabeled acetate in tumor cells have been conducted. Yoshimoto *et al*. examined [1-^{14}C]acetate uptake and metabolic fate under normoxia in four tumor cell lines including colon adenocarcinoma, nasal septum quasi-diploid tumor, ovary carcinoma, and melanoma as well as in a non-tumor fibroblast cell line to elucidate the implication of [1-^{11}C]acetate-PET imaging [22], and revealed that the tumor cells showed higher [1-^{14}C]acetate uptake than fibroblast cells under normoxia and that the tumor cells incorporated [1-^{14}C]acetate into lipids rather than CO_2 via the TCA cycle and amino acids. In addition, Hara *et al*. reported that [1-^{14}C]acetate uptake is accelerated under hypoxia in prostate cancer cells [23].

Concerning the gene expression of tumor ACSS, our previous study revealed that tumor cell lines, including Lewis lung carcinoma, LLC (LL/2); melanoma, B16; colon carcinoma, Colon (Colon-26); and mammary carcinoma, C127I, expressed little ACSS1, but greater cytosolic ACSS2 and that the expression of ACSS2 was up-regulated under hypoxia. We also found that ACSS2 plays an important role in hypoxic survival in tumor cells [24]. Interestingly, our data also demonstrated that ACSS2 participates in the reversible reaction between acetyl-CoA and acetate in tumor cells; i.e., ACSS2 is a bi-directional enzyme mediating a buffering role in tumor acetyl-CoA / acetate metabolism. These facts prompted us to hypothesize that ACSS2 might mediate uptake of radiolabeled acetate in tumor cells and that the uptake rate of radiolabeled acetate in tumor cells would be increased under hypoxia along with up-regulation of ACSS2 expression. In this study, to understand the uptake mechanism of radiolabeled acetate in tumor cells as a basis of tumor acetate PET, we characterized the patterns of [1-^{14}C]acetate uptake and ACSS2 expression in tumor cells and considered the role of tumor ACSS2 in the uptake of radiolabeled acetate.

2. Materials and methods

2.1. Cells and cultivation

Four mouse tumor cell lines were used in this study, LLC (LL/2) (CRL-1642, American Type Culture Collection or ATCC, mouse Lewis lung carcinoma), B16 (RCB1283, Riken Cell Bank, mouse melanoma), Colon (Colon-26; TKG 0518, Cell Resource Centre for Biomedical Research, Tohoku University, mouse colon carcinoma), and C127I (CRL-1616, ATCC, mouse mammary carcinoma). As a reference, a mouse fibroblast cell line, BALB/3T3 clone A31 (3T3; CCL-163, ATCC), was used. For the ACSS2 knock down study, tumor cells in which ACSS2 expression was inhibited by RNA interference (RNAi) were used. These RNAi tumor cells were previously constructed using lentiviral particles (Mission lentiviral

transduction particles; SHVRS-NM 019811; Sigma, Poole, UK) carrying expression cassettes encoding ACSS2-targeting single-hairpin RNA (shRNA). Non-targeting shRNA (SHC002V, Sigma) was also used as a negative control [24-26]. The cells were incubated in a humidified atmosphere of 5% CO_2 in air (normoxia) at 37 °C. Dulbecco's modified Eagle's medium (Invitrogen, Carlsbad, CA, USA) supplemented with 10% fetal bovine serum and antibiotics was used for growth. Exponentially growing cells were used for the experiments. Hypoxia (1.2% O_2, 93.8% N_2 and 5% CO_2) was achieved with a Personal Multi Gas Incubator (Astec, Fukuoka, Japan). The cells were trypsinized to detach them from the plates, and the number of viable cells was counted by the trypan blue dye-exclusion method.

2.2. [1-^{14}C]acetate uptake study

In this experiment, we optimized the number of cells for seeding to roughly control the number of cells present during the uptake study (LLC, B16, and Colon: 5×10^4, C127I: 8×10^4, 3T3: 1×10^5) in 1 ml growth medium per well in 24-well plates. The cells were incubated under normoxia for 24 h, and the cells for the hypoxic study were additionally pretreated with 2 h or 6 h hypoxia. After the preincubation, 500 μl growth medium containing 37 kBq of [1-^{14}C]acetate (2.07 GBq/mmol) (GE Healthcare, Pollards, UK) were added to each well, and the cells were incubated for 1 h under normoxia or hypoxia. We adopted a similar concentration of [1-^{14}C]acetate to that in Yoshimoto *et al*. [22]. Then, the medium was removed, and the cells were washed twice with ice-cold PBS. The resultant cells were lysed with 500 μl of 0.2N NaOH for 2 h at room temperature or processed by the Bligh and Dyer extraction method to separate the lipid- and water-soluble fractions [27]. The radioactivity of mixture of the lysate or separated fractions and a liquid scintillator (ACSII, GE Healthcare) was measured using a liquid scintillation counter (LSC-5000, Aloka, Tokyo, Japan). The number of cells treated before cell lysis was counted. In addition, the pretreatment with

long-term hypoxia (24 h) was also tested in the same manner.

2.3. Gene expression analysis.

Total RNA isolation was performed with a Micro-to-Midi total RNA purification system (Invitrogen). cDNA was synthesized from 1 μg of total RNA using the ReverTra Ace qPCR RT Kit (Toyobo, Osaka, Japan) and was subjected to real-time PCR. The real-time PCR was performed with Realtime PCR Master Mix (Toyobo) and TaqMan gene expression assays (Applied Biosystems, Foster City, CA, USA) using an ABI PRISM 7000 sequence detection system (Applied Biosystems) in total reaction volumes of 20 μl containing 10 μl Realtime PCR Master Mix, 9 μl 1/10 cDNA template, and 1 μl 20× TaqMan gene-expression assay (ACSS2, Mm00480101; β-actin, Mm00607939). PCR was carried out for 1 min at 95 °C, followed by 40 cycles at 95°C for 15 s and at 60°C for 1 min. ACSS2 mRNA was quantified by the comparative C_T method using β-actin expression as the endogenous control [28].

2.4. Statistical analysis.

Data are expressed as means and standard deviations. *P* values were calculated by the two-sided *t*-test for comparison between two groups. ANOVA was used for comparison between multiple treatment groups. *P* values < 0.05 were considered statistically significant. Values from four independent experiments are presented.

3. Results <Please locate Fig. 1 and Table 1 around here.>

3.1 [1-^{14}C]acetate uptake study

Fig. 1A shows [1-^{14}C]acetate uptake for 1 h in the cells examined. Under normoxic

conditions, all tumor cells showed higher [1-^{14}C]acetate uptake than the 3T3 fibroblast cells: 1.3-fold in LLC and B16, 1.6-fold in Colon, and 1.2-fold in C127I ($P < 0.001$ in Colon; $P < 0.01$ in LLC and C127I; $P < 0.02$ in B16). We also tested the [1-^{14}C]acetate uptake for 1 h under hypoxic conditions. In this study, the cells were treated with 2 h or 6 h hypoxia prior to the uptake study. In four all tumor cell lines, the [1-^{14}C]acetate uptake was much increased under hypoxia compared with normoxia; however, the 3T3 fibroblast cells did not show any increase in [1-^{14}C]acetate uptake under hypoxia. In the cells treated with 2 h hypoxia beforehand, the values were 1.3-fold, 1.2-fold, 1.6-fold, and 1.2-fold larger in LLC, B16, Colon, and C127I, respectively, compared with each cell type under normoxia ($P < 0.01$ in Colon and C127I; $P < 0.02$ in LLC and B16). Similarly, the cells treated with 6 h hypoxia beforehand showed increased [1-^{14}C]acetate uptake, compared with normoxia: 1.4-fold, 1.2-fold, 1.5-fold, and 1.4-fold larger than each cell type under normoxia in LLC, B16, Colon, and C127I, respectively ($P < 0.01$ in LLC, Colon, and C127I; $P < 0.04$ in B16). There was no significant difference between 2 h and 6 h hypoxic pre-treatments.

3.2 ACSS2 expression analysis

Fig. 1B shows the expression pattern of transcripts encoding cytosolic ACSS2 in the cells examined. The pattern of tumor ACSS2 expression resembled that of [1-^{14}C]acetate uptake. Namely, tumor ACSS2 expression showed an increase compared with that of the 3T3 fibroblast cells: 1.5-fold in LLC, 1.9-fold B16, 2.4-fold in Colon, and 2.2-fold in C127I, respectively ($P < 0.001$). Also, the expression of ACSS2 mRNA increased under hypoxia in tumor cells; whereas, it decreased in the 3T3 fibroblast cells. The values of ACSS2 expression were 1.4-fold and 1.6-fold larger in LLC, 1.5-fold and 1.1-fold larger in B16, 1.6-fold and 1.7-fold larger in Colon, and 1.1-fold and 1.6-fold larger in C127I, after 2h and 6h hypoxic treatment, respectively, compared with each cell type under normoxia ($P < 0.01$

in LLC, B16 and Colon; $P < 0.03$ in C127I).

3.3 Effect of long-term hypoxia to [1-^{14}C]acetate uptake and ACSS2 expression <Please locate Table 1 around here.>

Table 1 shows the ratios of the long-term hypoxic pretreatment (24 h) and short-term hypoxic pretreatment (2 h or 6 h) to normoxic treatment in the [1-^{14}C]acetate uptake and ACSS2 gene expression. In all tumor cell lines, cells pretreated with 24 h hypoxia showed significant increase of [1-^{14}C]acetate uptake and ACSS2 expression, compared with normoxia. This tendency was similar to that seen in the cells pretreated with 2 h or 6 h hypoxia.

3.4 Distribution ratio of radioactivity in fractions separated from tumor cells <Please locate Fig. 2 around here.>

The fate of the ^{14}C incorporated into tumor cells under normoxia or hypoxia was further examined. The ^{14}C incorporated into the tumor cells was mostly distributed in the lipid-soluble fraction: 81.6 % and 87.6 % in LLC, 70.2 % and 79.3 % in B16, 85.8 % and 91.4 % in Colon, and 74.1 % and 86.0 % in C127I of the total ^{14}C incorporated into the cells, under normoxia and hypoxia, respectively (Fig. 2). The proportion incorporated into the lipid-soluble fraction under hypoxia tended to be higher than that under normoxia, and the increase was significant in the LLC, Colon, and C127I cells ($P < 0.05$ in LLC; $P < 0.001$ in Colon and C127I); whereas, it was marginal and not significant in the B16 cells.

3.5 Involvement of ACSS2 in tumor [1-^{14}C]acetate uptake <Please locate Fig. 3 here.>

To test the involvement of ACSS2 in acetate tracer uptake in tumor cells, we examined [1-^{14}C]acetate uptake in RNAi cells derived from the four tumor cell lines. In the ACSS2-RNAi tumor cells, the expression of ACSS2 was decreased compared with

control-RNAi tumor cells in all the tumor cell lines examined (Fig. 3A-D, upper). Furthermore, in the ACSS2-RNAi tumor cells, knock down of ACSS2 caused a corresponding reduction in [1-^{14}C]acetate uptake in all examined tumor cell lines under normoxia (Fig. 3A-D, lower). Under hypoxic conditions, a similar tendency was also confirmed in all examined tumor cell lines (data not shown).

4. Discussion

We characterized [1-^{14}C]acetate uptake in tumor cells, including LLC, B16, Colon, and C127I cells. All the tumor cells we examined incorporated larger amounts of [1-^{14}C]acetate than the 3T3 fibroblast cells under normoxia. Our results showed concordance with a previous report by Yoshimoto *et al* that used other tumor cell lines. [22]. We also confirmed the acceleration of [1-^{14}C]acetate uptake under hypoxia in all tumor cell lines examined. Hara *et al*. reported an increase in [1-^{14}C]acetate uptake under hypoxia in prostate cancer cells [23]. Our results revealed a similar tendency.

In the present study, we found that the pattern of [1-^{14}C]acetate uptake resembled the pattern of cytosolic ACSS2 mRNA expression in the four tumor cell lines examined (Fig. 1 and Table 1). In addition, from the RNAi studies, we revealed that knockdown of ACSS2 in the tumor cells led to a corresponding reduction in [1-^{14}C]acetate uptake under normoxia and hypoxia, respectively. Taken together, it can be concluded that ACSS2 was involved in [1-^{14}C]acetate uptake in the tumor cells and that up-regulation of ACSS2 expression under hypoxia led to an increase in [1-^{14}C]acetate uptake.

Hara *et al*. demonstrated that prostate cancer cells pretreated with 4 h or 5 h hypoxia showed acceleration of [1-^{14}C]acetate uptake under hypoxia [23]. In this study, we used cells that were pretreated with 2 h or 6 h hypoxia for the uptake experiments to evaluate [1-^{14}C]acetate uptake under hypoxia. We found that in both hypoxic treatment groups of each

tumor cell, [1-^{14}C]acetate uptake and ACSS2 expression were increased under hypoxia, compared with normoxia. This indicates that the rate of [1-^{14}C]acetate uptake under hypoxia became faster than that under normoxia, which mirrors the activation of ACSS2 expression. Therefore, hypoxia induced the tumor cells to up-regulate ACSS2 expression and [1-^{14}C]acetate uptake within 2 h. Similarly, the long-term hypoxic treatment led to increase [1-^{14}C]acetate uptake and ACSS2 expression. This means that, in tumor cells under more chronic hypoxic conditions, the acceleration of [1-^{14}C]acetate uptake could be also caused by the up-regulation of ACSS2 expression.

We have previously reported that the tumor cells used in this study expressed cytosolic ACSS2 and that the expression of ACSS2 was increased under hypoxia; whereas, mitochondrial ACSS1 was little expressed regardless of the oxygen conditions [24]. In this study, we showed that tumor [1-^{14}C]acetate uptake reflected the expression of cytosolic ACSS2 and that the cytosolic ACSS2 was involved in [1-^{14}C]acetate uptake in these tumor cell lines. This indicates that the uptake of radiolabeled acetate reflects cytosolic ACSS2 activity rather than mitochondrial ACSS1 in these tumor cell lines. In contrast, it has been reported that in the myocardium mitochondrial ACSS1 is more highly expressed than ACSS2 and is involved in uptake of radiolabeled acetate [5]. This means that the uptake mechanism of radiolabeled acetate in tumor cells might be different from that in the myocardium. Furthermore, the metabolic fate of the incorporated acetate seems different between tumor cells and the myocardium; namely, tumor cells mainly metabolize radiolabeled acetate into lipids [22]; whereas, the myocardium mainly metabolizes it into CO_2 [5, 8-11].

ACSS2 is known to be highly expressed in the liver as a lipogenic enzyme that incorporates acetate into lipids [5, 29, 30]. On the other hand, our studies have demonstrated that ACSS2 can mediate the reversible reaction between acetyl-CoA and acetate in tumor cells ([24], this study). In this study, we administered 37 kBq of [1-^{14}C]acetate (2.07

GBq/mmol) to tumor cells, which can be estimated as a 3 – 9-fold larger amount of acetate compared with the level of tumor acetate excretion reported previously [24]. This suggests that the reactions of tumor ACSS2 are affected by the concentrations of acetate and acetyl-CoA.

Löffler and Schneider reported that, under hypoxia, the proportion of [U-^{14}C]acetate incorporated into lipids is increased in Ehrlich ascites tumor cells [31]. Similarly, this study showed that [1-^{14}C]acetate incorporation into the lipid-soluble fraction tended to be enhanced in tumor cells under hypoxia. On the other hand, Vāvere et al. showed that [1-^{11}C]acetate uptake is correlated with expression of fatty acid synthetase (FAS) by *in vitro* and *in vivo* study [32] and a recent study by Furuta et al. demonstrated that hypoxia up-regulates FAS via phosphorylation of Akt followed by activation of hypoxia-inducible factor 1 (HIF-1) in various types of tumor cells [33]. According to Furuta et al. [33], the expression of FAS is activated by H_2O_2 generation under hypoxia, and the up-regulation of FAS leads to hypoxia-induced chemoresistance in tumor cells, which suggests that fatty acid synthesis is activated under hypoxia to adapt to environments involving hypoxic stress in tumor cells. Taking these studies and our results together, it is reasonable to assume that the incorporated acetate in tumor cells under hypoxia is used for activated fatty acid synthesis and is stored in the lipid-soluble fractions of tumor cells. In other words, radiolabeled acetate would be a useful marker that indicates activated FAS expression under hypoxia.

Consequently, in this paper, we found that uptake of radiolabeled acetate reflects ACSS2 expression in tumor cells, which helps to elucidate the basis of tumor acetate PET. However, at this moment, our findings are limited to *in vitro* conditions. To further interpret tumor acetate PET, detailed information, such as on the metabolic fate of radiolabeled acetate *in vivo* and on the levels of acetate or acetyl-CoA in intact tumors, should be obtained.

Acknowledgments

We thank the staff of the Biomedical Imaging Research Centre of the University of Fukui, Japan, for their helpful discussion and H. Takagi and Y. Kishimoto for technical help. This work was supported in part by Grants-in-Aid for Young Scientists (B) from the Japan Society for the Promotion of Science, Japan (JSPS) (to Y.Y.); by Research for Promoting Techbological Seeds from Japan Science and Technology Agency, Japan (to Y.Y.); by the 21st Century Centers of Excellence (COE) program from the JSPS (to Y.F.); and a Grant-in-Aid for Tumor Research from the Ministry of Health, Labor, and Welfare of Japan (to Y.F.).

References

[1] Porenta G, Cherry S, Czernin J, Brunken R, Kuhle W, Hashimoto T, et al. Noninvasive determination of myocardial blood flow, oxygen consumption and efficiency in normal humans by carbon-11 acetate positron emission tomography imaging. Eur J Nucl Med 1999;26:1465-74.

[2] Schelbert HR. PET contributions to understanding normal and abnormal cardiac perfusion and metabolism. Annals of biomedical engineering 2000;28:922-9.

[3] Henes CG, Bergmann SR, Walsh MN, Sobel BE, Geltman EM. Assessment of myocardial oxidative metabolic reserve with positron emission tomography and carbon-11 acetate. J Nucl Med 1989;30:1489-99.

[4] Choi Y, Huang SC, Hawkins RA, Hoh CK, Krivokapich J, Buxton DB, et al. A refined method for quantification of myocardial oxygen consumption rate using mean transit time with carbon-11-acetate and dynamic PET. J Nucl Med 1993;34:2038-43.

[5] Fujino T, Kondo J, Ishikawa M, Morikawa K, Yamamoto TT. Acetyl-CoA synthetase 2, a mitochondrial matrix enzyme involved in the oxidation of acetate. J Biol Chem 2001;276:11420-6.

[6] Beinert H, Green DE, Hele P, Hift H, Von Korff RW, Ramakrishnan CV, et al. The acetate activating enzyme system of heart muscle. J Biol Chem 1953;203:35-45.

[7] Hele P. The acetate activating enzyme of beef heart. J Biol Chem 1954;206:671-6.

[8] Brown M, Marshall DR, Sobel BE, Bergmann SR. Delineation of myocardial oxygen utilization with carbon-11-labeled acetate. Circulation 1987;76:687-96.

[9] Buxton DB, Nienaber CA, Luxen A, Ratib O, Hansen H, Phelps ME, et al. Noninvasive quantitation of regional myocardial oxygen consumption *in vivo* with [1-^{11}C]acetate and dynamic positron emission tomography. Circulation 1989;79:134-42.

[10] Klein LJ, Visser FC, Knaapen P, Peters JH, Teule GJ, Visser CA, et al. Carbon-11 acetate as a tracer of myocardial oxygen consumption. Eur J Nucl Med 2001;28:651-68.

[11] Tamaki N, Magata Y, Takahashi N, Kawamoto M, Torizuka T, Yonekura Y, et al. Oxidative metabolism in the myocardium in normal subjects during dobutamine infusion. Eur J Nucl Med 1993;20:231-7.

[12] Oyama N, Akino H, Kanamaru H, Suzuki Y, Muramoto S, Yonekura Y, et al. ^{11}C-acetate PET imaging of prostate cancer. J Nucl Med 2002;43:181-6.

[13] Oyama N, Miller TR, Dehdashti F, Siegel BA, Fischer KC, Michalski JM, et al. ^{11}C-acetate PET imaging of prostate cancer: detection of recurrent disease at PSA relapse. J Nucl Med 2003;44:549-55.

[14] Shreve P, Chiao PC, Humes HD, Schwaiger M, Gross MD. Carbon-11-acetate PET imaging in renal disease. J Nucl Med 1995;36:1595-601.

[15] Ho CL, Yu SC, Yeung DW. ^{11}C-acetate PET imaging in hepatocellular carcinoma and other liver masses. J Nucl Med 2003;44:213-21.

[16] Liu RS, Chang CP, Chu LS, Chu YK, Hsieh HJ, Chang CW, et al. PET imaging of

brain astrocytoma with 1-^{11}C-acetate. Eur J Nucl Med Mol imaging 2006;33:420-7.

[17] Tsuchida T, Takeuchi H, Okazawa H, Tsujikawa T, Fujibayashi Y. Grading of brain glioma with 1-^{11}C-acetate PET: comparison with ^{18}F-FDG PET. Nucl Med Biol 2008;35:171-6.

[18] Lear JL, Ackermann RF. Evaluation of radiolabeled acetate and fluoroacetate as potential tracers of cerebral oxidative metabolism. Metabolic Brain Disease 1990;5:45-56.

[19] Sun LQ, Mori T, Dence CS, Ponde DE, Welch MJ, Furukawa T, et al. New approach to fully automated synthesis of sodium [^{18}F]fluoroacetate -- a simple and fast method using a commercial synthesizer. Nucl Med Biol 2006;33:153-8.

[20] Ponde DE, Dence CS, Oyama N, Kim J, Tai YC, Laforest R, et al. ^{18}F-fluoroacetate: a potential acetate analog for prostate tumor imaging--in vivo evaluation of ^{18}F-fluoroacetate versus ^{11}C-acetate. J Nucl Med 2007;48:420-8.

[21] Matthies A, Ezziddin S, Ulrich EM, Palmedo H, Biersack HJ, Bender H, et al. Imaging of prostate cancer metastases with ^{18}F-fluoroacetate using PET/CT. Eur J Nucl Med Mol imaging 2004;31:797.

[22] Yoshimoto M, Waki A, Yonekura Y, Sadato N, Murata T, Omata N, et al. Characterization of acetate metabolism in tumor cells in relation to cell proliferation: acetate metabolism in tumor cells. Nucl Med Biol 2001;28:117-22.

[23] Hara T, Bansal A, DeGrado TR. Effect of hypoxia on the uptake of [methyl-^{3}H]choline, [1-^{14}C] acetate and [^{18}F]FDG in cultured prostate cancer cells. Nucl Med Biol 2006;33:977-84.

[24] Yoshii Y, Furukawa T, Yoshii H, Mori T, Kiyono Y, Waki A, et al. Cytosolic acetyl-CoA synthetase affected tumor cell survival under hypoxia: the possible function in tumor acetyl-CoA/acetate metabolism. Cancer Sci 2009;100:821-7.

[25] Scholl C, Bansal D, Dohner K, Eiwen K, Huntly BJ, Lee BH, et al. The homeobox gene CDX2 is aberrantly expressed in most cases of acute myeloid leukemia and promotes leukemogenesis. J Clin Invest 2007;117:1037-48.

[26] Patel JH, McMahon SB. BCL2 is a downstream effector of MIZ-1 essential for blocking c-MYC-induced apoptosis. J Biol Chem 2007;282:5-13.

[27] Bligh EG, Dyer WJ. A rapid method of total lipid extraction and purification. Canadian J Biochem Physiol 1959;37:911-7.

[28] Livak KJ, Schmittgen TD. Analysis of relative gene expression data using real-time quantitative PCR and the $2^{-\Delta\Delta C_T}$ Method. Methods 2001;25:402-8.

[29] Sone H, Shimano H, Sakakura Y, Inoue N, Amemiya-Kudo M, Yahagi N, et al. Acetyl-coenzyme A synthetase is a lipogenic enzyme controlled by SREBP-1 and energy status. Am J Physiol 2002;282:E222-30.

[30] Luong A, Hannah VC, Brown MS, Goldstein JL. Molecular characterization of human acetyl-CoA synthetase, an enzyme regulated by sterol regulatory element-binding proteins. J Biol Chem 2000;275:26458-66.

[31] Loffler M, Schneider F. Lipogenesis in Ehrlich ascites tumor cells under anaerobic culture conditions. J Cancer Res Clin Oncol 1979;95:115-22.

[32] Vavere AL, Kridel SJ, Wheeler FB, Lewis JS. 1-^{11}C-acetate as a PET radiopharmaceutical for imaging fatty acid synthase expression in prostate cancer. J Nucl Med 2008;49:327-34.

[33] Furuta E, Pai SK, Zhan R, Bandyopadhyay S, Watabe M, Mo YY, et al. Fatty acid synthase gene is up-regulated by hypoxia via activation of Akt and sterol regulatory element binding protein-1. Cancer Res 2008;68:1003-11.

Figure Legends

Fig. 1. [1-^{14}C]acetate uptake (A) and ACSS2 mRNA expression (B) in tumor cells (LLC, B16, Colon, and C127I) and fibroblast cells (3T3) under normoxia and in the same cells under hypoxia after pretreatment with 2 h hypoxia or 6 h hypoxia. (A) [1-^{14}C]acetate uptake in the tumor cells was higher than in the 3T3 cells under normoxia (* $P < 0.02$, ** $P < 0.01$, *** $P < 0.001$). [1-^{14}C]acetate uptake in the tumor cells increased under hypoxia (†$P < 0.04$, †† $P < 0.02$, ††† $P < 0.01$), but not in 3T3. NS = not significant. (B) ACSS2 expression under normoxia was higher in the tumor cells compared with the 3T3 cells (P * < 0.001). The values were increased under hypoxia in the tumor cells, but decreased in the 3T3 cells († < 0.03, †† < 0.01, ††† < 0.001).

Fig. 2. Distribution of incorporated ^{14}C into the lipid- and water-soluble fractions of tumor cells (LLC, B16, Colon, and C127I cells) after [1-^{14}C]acetate uptake. The asterisks indicate the statistical significance between normoxia and hypoxia (* $P < 0.05$, ** $P < 0.001$). The data indicates the proportion of ^{14}C radioactivity in the lipid-soluble fractions (gray areas) and water-soluble fractions (white areas).

Fig. 3. ACSS2 knockdown decreased [1-^{14}C]acetate uptake in tumor cells (LLC, B16, Colon, and C127I). The asterisks indicate statistical significance (* $P < 0.01$, ** $P < 0.005$, *** $P < 0.001$). The data indicates the percentages of ACSS2 mRNA expression (upper) and ^{14}C incorporation (lower) in ACSS2-RNAi tumor cells relative to control-RNAi tumor cells in LLC (A), B16 (B), Colon (C), and C127I cells (D) under normoxia.

Table 1 Effect of long-term (24 h) and short-term (2 h or 6 h) hypoxia in the [1-^{14}C]acetate uptake and ACSS2 gene expression

Cell line	Treatment	Ratio to each normoxic treatment	
		[1-^{14}C] acetate uptake	Acss2 gene expression
LLC	Normoxia	1.00 ± 0.06[a]	1.00 ± 0.15[a]
	Hypoxia with 2 h pretreatment	1.29 ± 0.14[b]	1.42 ± 0.18[b]
	Hypoxia with 6 h pretreatment	1.36 ± 0.07[b]	1.63 ± 0.25[b]
	Hypoxia with 24 h pretreatment	1.73 ± 0.29[b]	1.81 ± 0.07[b]
B16	Normoxia	1.00 ± 0.10[a]	1.00 ± 0.09[a]
	Hypoxia with 2 h pretreatment	1.22 ± 0.07[b]	1.46 ± 0.03[b]
	Hypoxia with 6 h pretreatment	1.17 ± 0.05[b]	1.14 ± 0.05[c]
	Hypoxia with 24 h pretreatment	1.64 ± 0.08[c]	1.98 ± 0.20[d]
Colon	Normoxia	1.00 ± 0.09[a]	1.00 ± 0.32[a]
	Hypoxia with 2 h pretreatment	1.56 ± 0.18[b]	1.59 ± 0.07[b]
	Hypoxia with 6 h pretreatment	1.53 ± 0.07[b]	1.71 ± 0.14[b]
	Hypoxia with 24 h pretreatment	1.81 ± 0.04[c]	3.28 ± 1.56[b]
C127I	Normoxia	1.00 ± 0.04[a]	1.00 ± 0.03[a]
	Hypoxia with 2 h pretreatment	1.17 ± 0.06[b]	1.12 ± 0.04[b]
	Hypoxia with 6 h pretreatment	1.43 ± 0.18[b]	1.62 ± 0.35[b]
	Hypoxia with 6 h pretreatment	2.05 ± 0.11[c]	2.58 ± 0.86[b]

3T3	Normoxia	1.00 ± 0.04	1.00 ± 0.05
	Hypoxia with 2 h pretreatment	0.96 ± 0.07	0.59 ± 0.12
	Hypoxia with 6 h pretreatment	0.91 ± 0.04	0.33 ± 0.08
	Hypoxia with 24 h pretreatment	0.71 ± 0.05	1.09 ± 0.54

[a-d] The significant differences are shown by different letters on each group ($P < 0.05$).

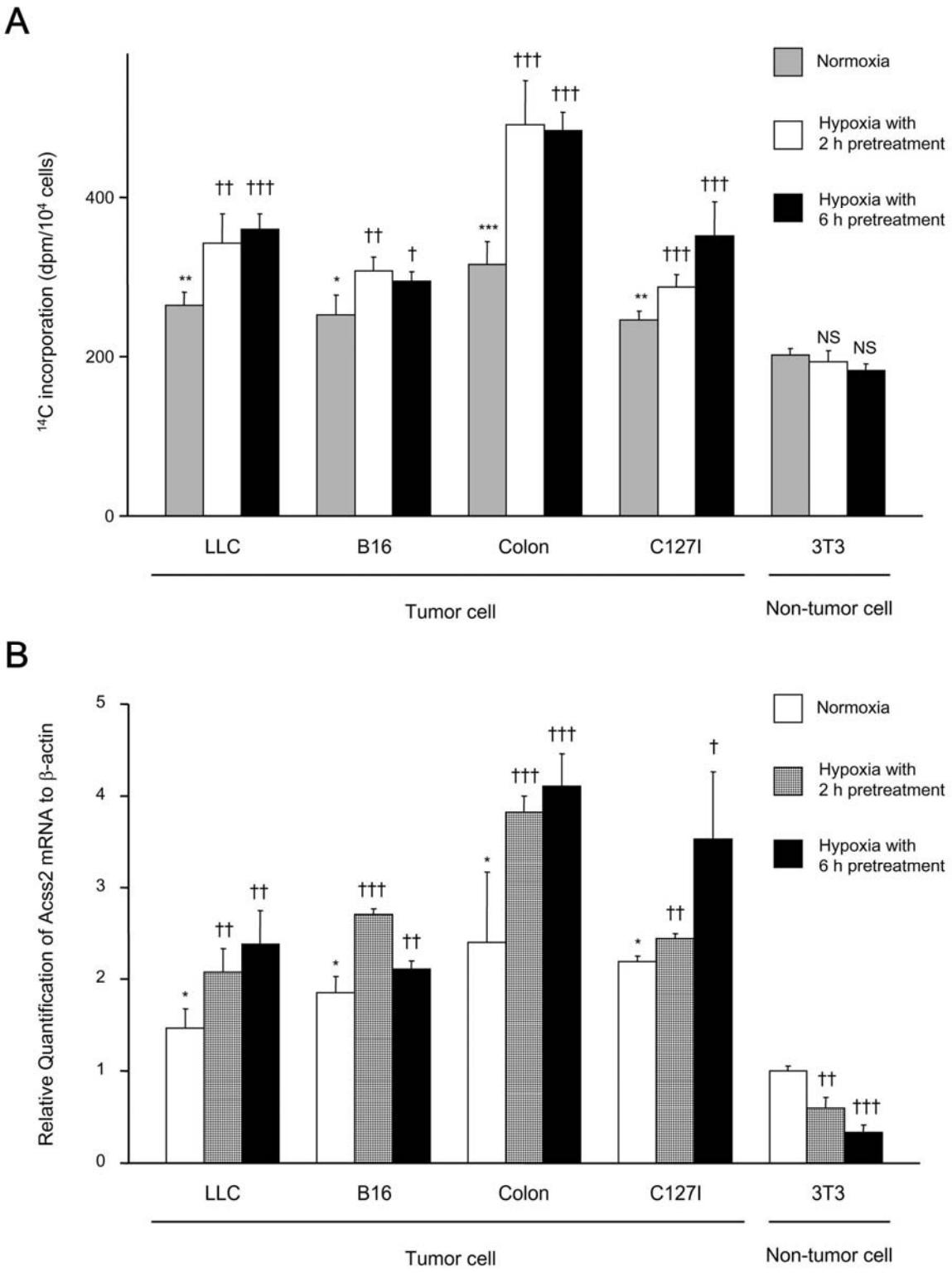
A
^{14}C incorporation (dpm/10^4 cells)
400
200
0
Normoxia
Hypoxia with 2 h pretreatment
Hypoxia with 6 h pretreatment
LLC
B16
Colon
C127I
3T3
Tumor cell
Non-tumor cell
NS
B
Relative Quantification of Acss2 mRNA to β-actin
5
4
3
2
1
0

Fig.1

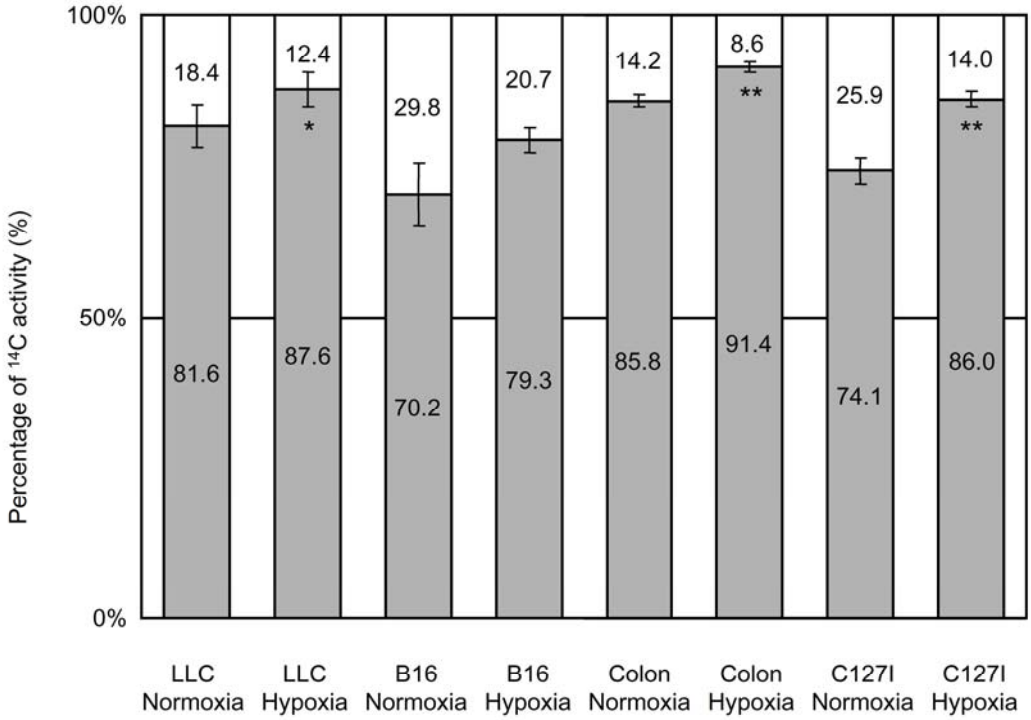
100%
50%
0%
Percentage of ¹⁴C activity (%)
18.4
81.6
12.4
*
87.6
29.8
70.2
20.7
79.3
14.2
85.8
8.6
**
91.4
25.9
74.1
14.0
**
86.0
LLC Normoxia
LLC Hypoxia
B16 Normoxia
B16 Hypoxia
Colon Normoxia
Colon Hypoxia
C127I Normoxia
C127I Hypoxia

Fig.2

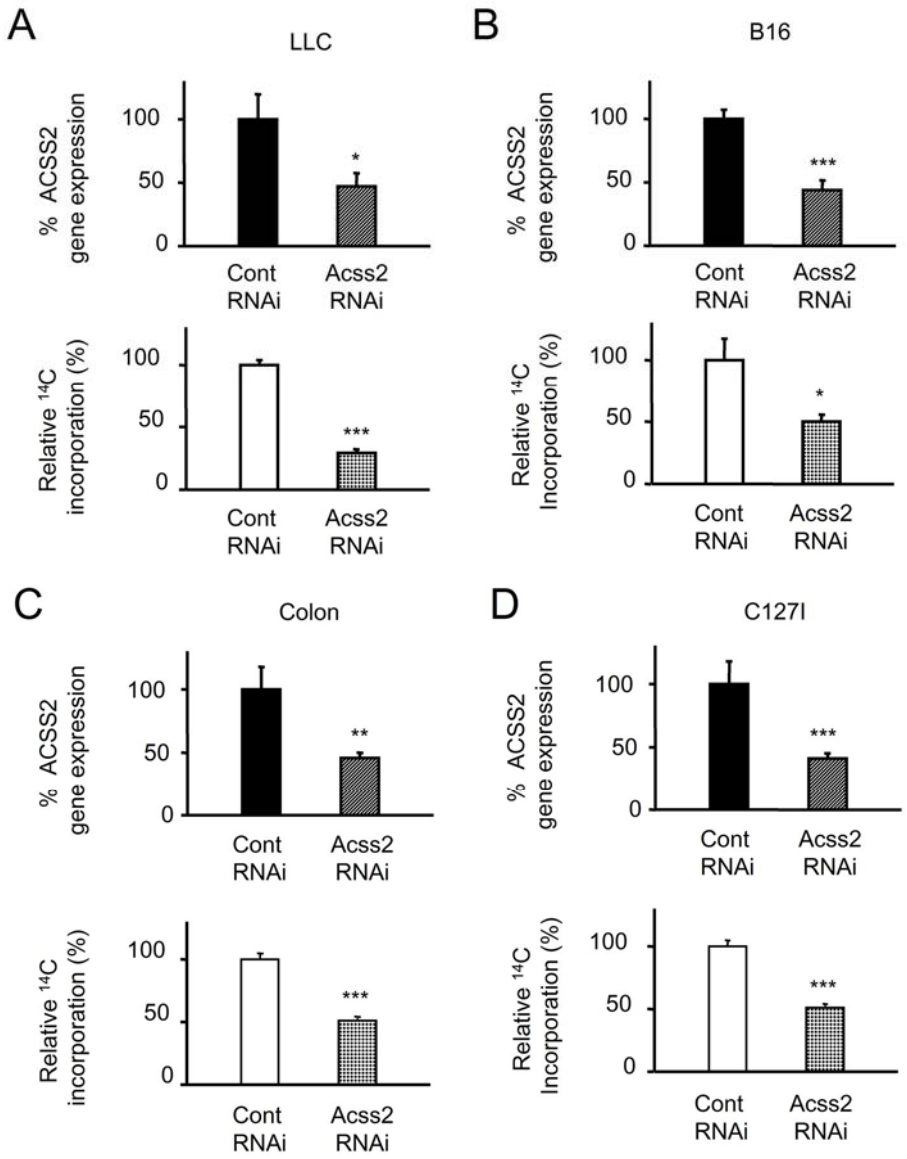
A
LLC
% ACSS2 gene expression
100
50
0
*
Cont RNAi
Acss2 RNAi
Relative ¹⁴C incorporation (%)
100
50
0
***
Cont RNAi
Acss2 RNAi
B
B16
% ACSS2 gene expression
100
50
0
***
Cont RNAi
Acss2 RNAi
Relative ¹⁴C Incorporation (%)
100
50
0
*
Cont RNAi
Acss2 RNAi
C
Colon
% ACSS2 gene expression
100
50
0
**
Cont RNAi
Acss2 RNAi
Relative ¹⁴C incorporation (%)
100
50
0
***
Cont RNAi
Acss2 RNAi
D
C127I
% ACSS2 gene expression
100
50
0
***
Cont RNAi
Acss2 RNAi
Relative ¹⁴C Incorporation (%)
100
50
0
***
Cont RNAi
Acss2 RNAi

Fig.3